



# Molar mass dependence of structure of xanthan thermally denatured and renatured in dilute solution

Yasuhiro Matsuda<sup>1</sup> · Kazuya Okumura<sup>1</sup> · Shigeru Tasaka<sup>1</sup>

Received: 5 March 2018 / Revised: 4 June 2018 / Accepted: 6 June 2018 / Published online: 3 July 2018  
© The Society of Polymer Science, Japan 2018

## Abstract

Double helical polysaccharide, xanthan samples with varying molar mass were thermally denatured and renatured in dilute solutions. Both the weight average molar mass, which was determined by size exclusion chromatography (SEC), and viscosity average molar mass decreased after denaturation and renaturation for samples with an initial molar mass of  $10^6$  g mol<sup>-1</sup>, but those for the samples with an initial molar mass of  $10^5$  or  $10^7$  g mol<sup>-1</sup> decreased only slightly. Although the double helices of xanthan only partially dissociated into single chains, the molar mass distribution estimated by SEC did not broaden drastically by the denaturation and renaturation. These results can be explained by the formation of hairpin structures by the single chains, which are restricted to xanthan with a molar mass of  $10^5$  g mol<sup>-1</sup> by the strain of the hairpin loop, and for xanthan molar masses of  $10^7$  g mol<sup>-1</sup> by the incomplete dissociation of its long polymer chains.

## Introduction

Xanthan is a double-helical polysaccharide used to control viscosity in foods and cosmetics [1]. The double helical structure provides rigidity to the main chains of xanthan, which has a persistence length of 100–120 nm, and these rigid main chains enhance the viscosity of aqueous solutions [2–4]. It is known that the double helices can be unwound in aqueous solutions with low ionic strengths at high temperature (denaturation) and rewound in solutions with high ionic strengths at low temperature (renaturation).

Because products containing xanthan can be exposed to temperature changes during processes such as cooking, the denaturation and renaturation behaviors of xanthan are important for its application. Liu et al. [5, 6] carried out static light scattering and intrinsic viscosity measurements for xanthan in a 0.01 M aqueous solution of sodium

chloride heated at 80 °C, and concluded that the double helices of xanthan were partially unwound from their ends (the model in Fig. 1b was illustrated according to their proposed model). On the other hand, Capron et al. [7] reported that a double-helical dimer of xanthan dissociated into two free coils, and each coil formed a hairpin structure with a half molar mass as that before denaturation. However, Oviatt and Brant [8] argued that aggregates of renatured xanthan formed due to the increased viscosity of its solution. These results seem to contradict each other.

To elucidate the structural change of xanthan that are induced by denaturation and renaturation, we prepared xanthan samples with molar masses of  $0.12\text{--}1.4 \times 10^6$  g mol<sup>-1</sup> in the native state by sonication and fractionation, and denatured and renatured the samples under various conditions [9]. The structural changes were investigated by circular dichroism (CD) spectroscopy and size exclusion chromatography-on line multi angle light scattering (SEC-MALS). While the CD spectra of the renatured samples were very similar to those of the native ones, the molar mass increased when the samples were denatured and renatured in solutions with high xanthan and salt concentrations, and the molar mass after the renaturation was approximately half as that of the native state when the samples were denatured and renatured in solutions containing low xanthan and salt concentrations. An increase in the radius of gyration was also detected for xanthan samples that were denatured and renatured in concentrated solutions, but was not remarkable comparing

**Electronic supplementary material** The online version of this article (<https://doi.org/10.1038/s41428-018-0098-7>) contains supplementary material, which is available to authorized users.

✉ Yasuhiro Matsuda  
matsuda.yasuhiro@shizuoka.ac.jp

<sup>1</sup> Department of Applied Chemistry and Biochemical Engineering, Shizuoka University, 3-5-1 Johoku, Naka-ku, Hamamatsu 432-8561, Japan

the increase in the molar mass, which suggests the formation of branched structures.

Based on the experimental results described above, a model describing the structural changes of xanthan was proposed and is as shown in Fig. 1. When xanthan is denatured in concentrated solution, the double helices only partially unwind (Fig. 1b). Renaturation induces inter-dimer rewinding (between the coil 1 and coil 2, and coil 3 and coil 4), and the formation of aggregates, as shown in Fig. 1c. On the other hand, when xanthan is denatured in dilute solution, the double helices dissociate into two free coils (Fig. 1d), which form helices with a hairpin structure during renaturation (Fig. 1e). Atomic force microscopy (AFM) of the renatured xanthan samples supported the model shown in Fig. 1 [10]. A branched helical structure, like Fig. 1c [11] and a hairpin structure like Fig. 1e [12], which are formed by unwinding and rewinding the helices, have already been reported for DNA.

The model illustrated in Fig. 1 indicates that the structure of xanthan formed by denaturation and renaturation is not uniform, but can be changeable by the solution conditions. This complicated behavior is one of the factors preventing a comprehensive understanding of the denaturation and renaturation of xanthan. Although there has been some research investigating the denaturation and renaturation of xanthan considering that it is changeable to the solution conditions using various analyses such as viscoelastic measurements [13], particle tracking microrheology [14], and AFM [15, 16], structural changes of xanthan induced by denaturation and renaturation is still under discussion.

In our previous study mentioned above, xanthan samples of which molar masses were decreased by sonication, were used because it is difficult to measure polymer samples with very high molar masses. However, because decreasing the molar mass of xanthan also decreases its ability to enhance the viscosity of a solution, xanthan is used industrially without decreasing its molar mass. We recently carried out static light scattering and intrinsic viscosity measurements for xanthan samples with a wider range of molar masses including a sample without sonication, after they were

denatured and renatured in concentrated solution [17]. When the molar mass of xanthan was very high, the molar mass, radius of gyration, and intrinsic viscosity increased only slightly by the renaturation. This behavior can be explained by assuming that intra-dimer renaturation (rewinding between coil 1 and coil 3, and coil 2 and coil 4 in Fig. 1b) rather than inter-dimer renaturation occurred, because xanthan samples with higher molar masses have lower transition mobility.

In this manuscript, we focused on the molar mass dependence of the structural changes of xanthan samples that were denatured and renatured in dilute solution, because xanthan is often used in dilute solutions [18]. Because the concentration for denaturation and renaturation in this study was too low for the light scattering instrument in our laboratory, size exclusion chromatography (SEC) with an ultraviolet detector was conducted to estimate the molar mass.

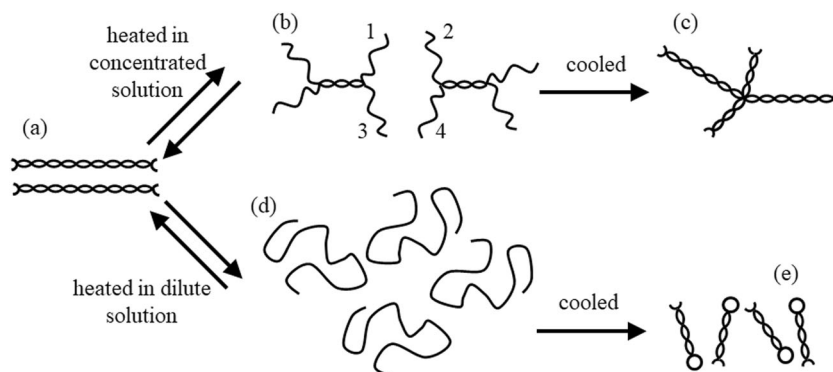
## Experimental procedure

The xanthan samples used in our previous study were also used in this report. The preparation procedures for the solutions was same except for the concentrations of xanthan and sodium chloride in our previous paper, which describes the details of the sample preparation [17].

One sample with a weight average molar mass  $M_w$  of  $4.65 \times 10^6 \text{ g mol}^{-1}$  was purchased from Tokyo Kasei Kogyo and used without decreasing molar mass. The other samples were kindly provided by Prof. Takahiro Sato at Osaka University. These samples were prepared by sonication, purification, fractionation, and neutralization, details of which are described in his previous report [2]. All the samples were dissolved in an aqueous solution containing 0.01 M of sodium chloride, neutralized with dilute aqueous solutions of chloric acid and sodium hydroxide, and precipitated in acetone.

To prepare “native xanthan” solutions, dried samples were dissolved in an aqueous solution containing 0.01 M of

**Fig. 1** Schematic images of native, denatured, and renatured xanthan proposed in our previous paper [9]



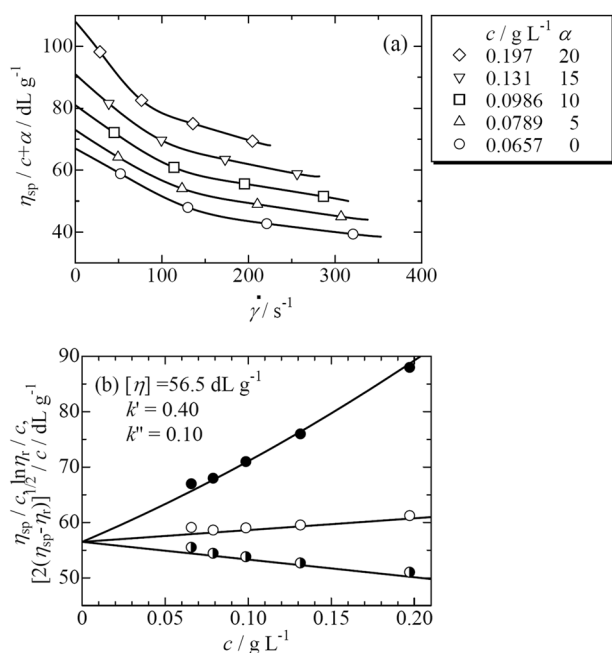


**Fig. 2** A typical result of intrinsic viscosity measurements for xanthan samples with high molar masses. ( $M_w = 4.65 \times 10^6 \text{ g mol}^{-1}$ ) **(a)** shear rate dependence of the solutions and **(b)** concentration dependence of the zero shear viscosities of the solutions. The data points in **a** are shifted vertically with  $\alpha$  shown in the figure

sodium chloride, and stirred for more than 24 h before measurements. “Renatured xanthan” solutions were prepared as follows. First, dried xanthan samples were dissolved in water purified using a Millipore Direct-Q with an electric resistivity of approximately 18 M $\Omega$  cm. The solutions were heated at 80 °C for 1 or 2 h by immersing the solutions in a water bath. After heating, sodium chloride was added to the solutions to fix its concentration to be 0.01 M. After stirring the solutions at room temperature for 24 h, they were diluted with an aqueous solution containing 0.01 M sodium chloride when the concentration was too high for the measurements. In the following, we will show the results for the solutions renatured at 1.0 g L $^{-1}$  of xanthan and heated for an hour unless described explicitly.

The CD spectrometer and the measurement conditions in this study were same as those in our previous study [17]. The denatured solution was prepared by dissolving xanthan samples into pure water, and measured at 80 °C. The native and renatured solutions were measured at 25 °C. The xanthan concentration for all the samples was fixed at 0.5 g L $^{-1}$ .

A conventional Ubbelohde type capillary viscometer and a four-bulb spiral capillary viscometer were used to determine the intrinsic viscosities  $[\eta]$  of the samples with molar masses lower than  $10^6 \text{ g mol}^{-1}$  and those with molar masses higher than  $10^6 \text{ g mol}^{-1}$ , respectively. All the measurements were carried out at 25 °C. The viscometers and the measurement conditions were same as those in our previous

paper [17]. Viscosity average molar mass  $M_v$  was calculated from  $[\eta]$  and the molar mass dependence of  $[\eta]$  for native xanthan, which was reported by Sato et al. [2–4].

As shown in the following section, the CD spectrum of renatured xanthan was very similar to that of native xanthan, which showed that the double helical structure of renatured xanthan was essentially identical to that of the native xanthan. This suggests that the persistence length and molar mass per contour length of the renatured xanthan, which determine the molar mass dependence of the intrinsic viscosity, are essentially identical to that of the native xanthan. The CD spectra did not disprove the existence of branched aggregates, as shown in Fig. 1 (c), and the branched structures can affect the molar mass dependence of the intrinsic viscosity. However, as shown in the following section, the intrinsic viscosity and molar mass estimated by SEC for renatured xanthan were comparable or smaller than those for native xanthan under the denaturation and renaturation conditions used in this study, which suggests that the amount of the branched aggregates is low in the renatured xanthan samples. We used the molar mass dependence of  $[\eta]$  for native xanthan to calculate  $M_v$  for all the renatured samples.

SEC was carried out with a Tosoh HPLC-8020 system equipped with a UV-8020 ultraviolet detector. The detection wavelength was 230 nm. An aqueous solution containing 0.01 M of sodium chloride was eluted at 0.5 ml min $^{-1}$  at 40 °C. One guard column (TSKguardcolumn PW $_{XL}$ ) and two separation columns (TSKgel GMPW $_{XL}$ ) were connected in series. The exclusion limit molecular weight of the separation columns was  $10^7$  for dextran. All the columns were products of Tosoh. Sample solutions were diluted to 0.2–0.3 g L $^{-1}$  of xanthan, and filtered through hydrophilic polytetrafluoroethylene filter units with pore size of 0.45  $\mu\text{m}$ .

The xanthan samples of which  $M_w$  at native state were determined by static light scattering in our previous study [17], were used to create the calibration curve, which was calculated to make the  $M_w$  measured by SEC to agree with those measured by static light scattering. Because elution time is determined by the dimension of polymers which is affected not only by molar mass but also by the degree of branching, the molar mass of the branched aggregates of xanthan as shown in Fig. 1c cannot be estimated correctly by using the calibration curve calculated above. However, for the same reason mentioned in the calculation of  $M_v$ , we used the calibration curves determined for the native samples for all of the renatured samples.

## Results

CD spectra of the native, denatured, and renatured xanthan samples with different molar masses are shown in Fig. S1 in

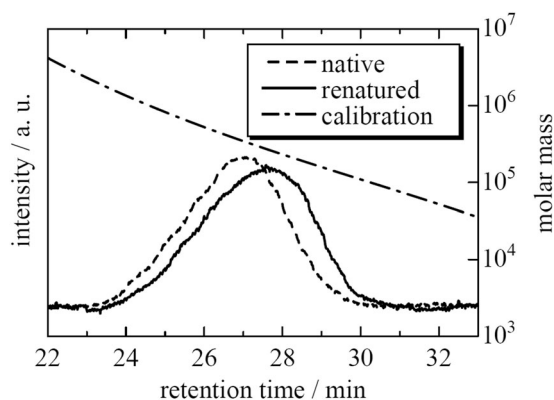


**Fig. 3** A typical result of SEC measurements for native and renatured xanthan samples ( $M_w = 4.85 \times 10^5 \text{ g mol}^{-1}$ ) and the calibration curve to calculate molar mass

the supplementary data. Whereas the spectra of denatured xanthan differ from those for native xanthan, the spectra for renatured xanthan were very similar to those for native xanthan. These results indicate that double helices unwound during the denaturation, but the local structure of the renatured xanthan was recovered that of native xanthan under the conditions used in this study. No distinct dependence of molar mass was detected for the local structural change induced by denaturation and renaturation. Similar local structural changes of xanthan induced by the denaturation and renaturation was also detected in our previous studies [9, 17].

Figure 2 shows a typical result of  $[\eta]$  measurements of the renatured xanthan samples with high molar mass. A typical results of  $[\eta]$  measurements for renatured xanthan samples with low molar mass is shown in Fig. S2 in the supplementary data. The  $[\eta]$  of both samples were smaller than the respective native samples, which were determined in our previous paper [17]. These results indicate that a part of the xanthan dimers dissociated into single chains during the denaturation, as shown in Fig. 1d, and formed a hairpin structure during the renaturation as shown in Fig. 1e. The Huggins coefficients  $k'$  were obtained as shown in the figures, and are normal, which suggest that  $[\eta]$  was determined successfully.

Figure 3 shows typical SEC curves for the native and renatured xanthan. The peak shifted to a longer retention time, which is consistent with a decrease in  $[\eta]$ . It should be noted that the peak for renatured xanthan was only slightly broader than that of the native sample.

Similar results as shown in Figs. 2–3 were obtained for xanthan samples with different molar masses, and their results are summarized in Fig. 4. The ordinate indicates the ratio of  $M_w$  or  $M_v$  of renatured xanthan to that of native one, and the abscissa is  $M_w$  at the native state. The subscripts “na” and “re” indicate native and renatured, respectively. The result obtained by SEC-MALS for xanthan with  $M_w$  of

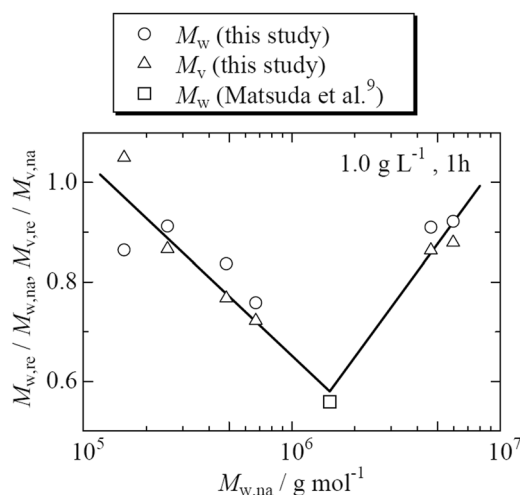


**Fig. 4** Ratios of  $M_w$  and  $M_v$  of renatured xanthan to those of native xanthan. The solutions with concentration of  $1.0 \text{ g L}^{-1}$  were heated for 1 h for denaturation. The line is for eye guide

$1.52 \times 10^6 \text{ g mol}^{-1}$  in our previous paper [9] is also shown in the figure. The solution with  $1.0 \text{ g L}^{-1}$  of xanthan was heated at  $80^\circ\text{C}$  for 2 h, and renatured at  $0.50 \text{ g L}^{-1}$  in the previous paper. The figure indicate that the molar mass of renatured xanthan decreased to the half value for the samples with a  $M_w$  of  $10^6 \text{ g mol}^{-1}$  in the native state, but was only slightly smaller than that of native xanthan for the samples with  $M_w$  of  $10^5$  or  $10^7 \text{ g mol}^{-1}$  in the native state.

To promote the dissociation of xanthan dimers into single chains, similar measurements were carried out with solutions heated for a longer time (2 h) and at a lower concentration ( $0.2 \text{ g L}^{-1}$ ). Because the solutions at  $0.2 \text{ g L}^{-1}$  were too dilute for  $[\eta]$  measurements, we gave up to determine  $M_v$  for this solution. The results are summarized in Figs. S3 and S4 in the supplementary data. No distinct change of the ratios of  $M_w$  and  $M_v$  were detected for the concentrations and heating times that we tried in this study.

## Discussion

Figure 4 indicates that the molar mass of the xanthan sample with the molar mass of  $10^6 \text{ g mol}^{-1}$  in the native state decreased by half by the denaturation and renaturation, while it decreased only slightly for xanthan samples with a molar mass of  $10^5$  or  $10^7 \text{ g mol}^{-1}$ . The proposed model for this behavior is shown in Fig. 5. When a xanthan dimer has a high molar mass and a long double helix, the dissociation into two free coils is suppressed because the dissociation requires complete unwinding of the double helix. For the xanthan samples with the molar mass of  $10^7 \text{ g mol}^{-1}$  in the native state, the double helices of the xanthan dimers partially unwound during the denaturation, and the unwound coils recover their original structure during the renaturation.

**Fig. 5** Schematic images of native, denatured, and renatured xanthan with various molar masses in dilute solutions

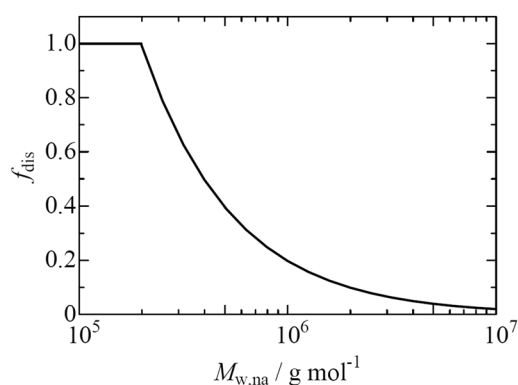
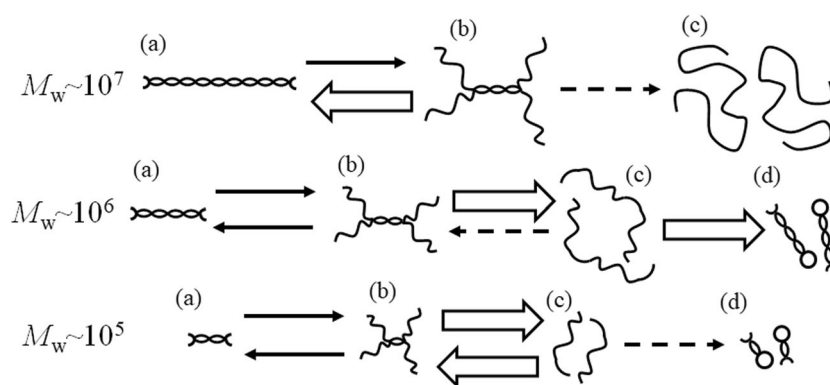


**Fig. 6** Molar mass dependence of the fraction of the xanthan chain distorted to form a hairpin loop to the whole chain

When a xanthan dimer has a low molar mass and a short double helix, it is dissociated into two free coils during the denaturation, but the formation of the hairpin structures is suppressed during the renaturation. The suppression of the hairpin structure formation is caused by the rigidity of the free coils of xanthan. Liu et al. [5, 6] estimated the persistence length of the unwound coils  $q_{\text{coil}}$  to be 21 nm, and the molar mass per contour length  $M_{L,\text{coil}}$  to be  $750 \text{ nm}^{-1}$  by fitting the radius of gyration and  $[\eta]$  determined experimentally for denatured xanthan to those calculated assuming the model shown in Fig. 1b. This value of the persistence length indicates that the free coils of xanthan are not flexible, but semi-flexible. Instead of forming the unstable hairpin loop, the coils are rewound into double helices with other coils to recover the original structure.

To avoid distortion caused by the formation of the hairpin loops, the coils have to form circles with radii longer than  $q_{\text{coil}}$  (21 nm). The circumference of a circle with a radius of  $q_{\text{coil}}$  divided by the contour length of the dissociated coils is defined as  $f_{\text{dis}}$ , and can be calculated using molar mass at native state  $M_w$  as follows:

$$f_{\text{dis}} \equiv \frac{2\pi q_{\text{coil}}}{M_w / (2M_{L,\text{coil}})} \quad (1)$$

When the circumference is longer than the contour length,  $f_{\text{dis}}$  is defined as 1. While  $f_{\text{dis}}$  was 1 below the molar mass  $1.98 \times 10^5 \text{ g mol}^{-1}$  in the native state, and remained well below the molar mass of  $5 \times 10^5 \text{ g mol}^{-1}$  in the native state, it became low around the molar mass of  $10^6 \text{ g mol}^{-1}$  in native state. The decrease of  $f_{\text{dis}}$  with an increase of the molar mass suggests that the slight decrease of the molar mass by the denaturation and renaturation was caused by the instability of the hairpin loop for xanthan with the molar mass of  $10^5 \text{ g mol}^{-1}$  in the native state. (See Fig. 6)

The assumption that xanthan with a molar mass of  $10^5 \text{ g mol}^{-1}$  in the native state tends to recover its double helical structure, and to form the hairpin structures with an increase of the molar mass, can explain the narrow molar mass distribution of the renatured xanthan measured by SEC shown in Fig. 3. To calculate the molar mass distributions, we introduced a parameter denoting the rate of dissociation,  $r_{\text{dis}}$ . It is assumed that the probability for a xanthan dimer to dissociate into two coils with a half molar mass is  $r_{\text{dis}}$ , and that to recover the original structure with the same molar mass is  $1-r_{\text{dis}}$ . The parameter  $r_{\text{dis}}$  was determined to best fit the calculated molar mass distribution determined by the SEC measurements.

The molar mass distribution was calculated by assuming two types of molar mass dependence of  $r_{\text{dis}}$  as shown in the upper part of Fig. 7. The lower part of Fig. 7 summarizes the typical molar mass distributions; determined by the SEC measurements, calculated by assuming  $r_{\text{dis}}$  is independent from the molar mass, and calculated by assuming  $r_{\text{dis}}$  is dependent on molar mass, as shown in the upper part. It clearly shows that the molar mass distribution calculated by assuming the variable  $r_{\text{dis}}$  fits the distribution determined by the SEC measurements, while the distribution calculated by assuming constant  $r_{\text{dis}}$  was significantly broader than the one determined by the SEC measurements.

Molar mass distribution was also calculated for the other xanthan samples, and summarized in Fig. 8. The ordinates indicate the ratio of  $M_w$  to the number average molar mass

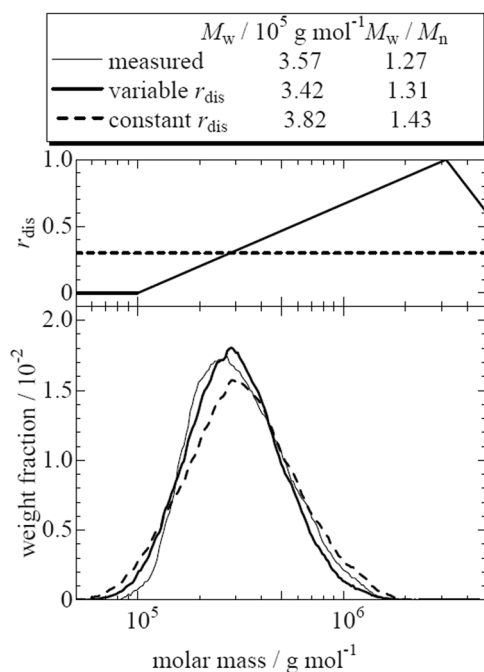


**Fig. 7** A typical molar mass distribution of renatured xanthan determined by a SEC measurement and those calculated by assuming variable  $r_{\text{dis}}$  and constant  $r_{\text{dis}}$  ( $M_w = 4.85 \times 10^5 \text{ g mol}^{-1}$ ). See the text for the details of the calculations

$M_n$ . Unfortunately, the molar mass distribution could not be determined precisely for two samples with high molar masses because of a tailing effect. As shown in Fig. 8, the molar mass distribution calculated by assuming the variable  $r_{\text{dis}}$  agreed well with that measured by SEC, while that calculated by assuming the constant  $r_{\text{dis}}$  was broader than that measured by SEC. This result also supports the molar mass dependence of the denaturation and renaturation behaviors, as proposed in Fig. 5.

## Conclusion

The thermally denaturation and renaturation behaviors of xanthan samples with various molar masses in dilute solutions were investigated. Both  $M_w$  as determined by SEC measurements and  $M_v$  as determined by  $[\eta]$  measurements indicated that the molar mass decreased only slightly for xanthan samples with a molar mass of  $10^5$  and  $10^7 \text{ g mol}^{-1}$  by denaturation and renaturation, while it decreased by half for xanthan samples with an initial molar mass of  $10^6 \text{ g mol}^{-1}$ . The suppression of the decrease can be caused by the long double helices for xanthan samples with molar mass of  $10^7 \text{ g mol}^{-1}$ , and by the instability of the hairpin loop for xanthan samples with molar mass of  $10^5 \text{ g mol}^{-1}$ . This model is supported by the molar mass distribution of the renatured xanthan determined by SEC.

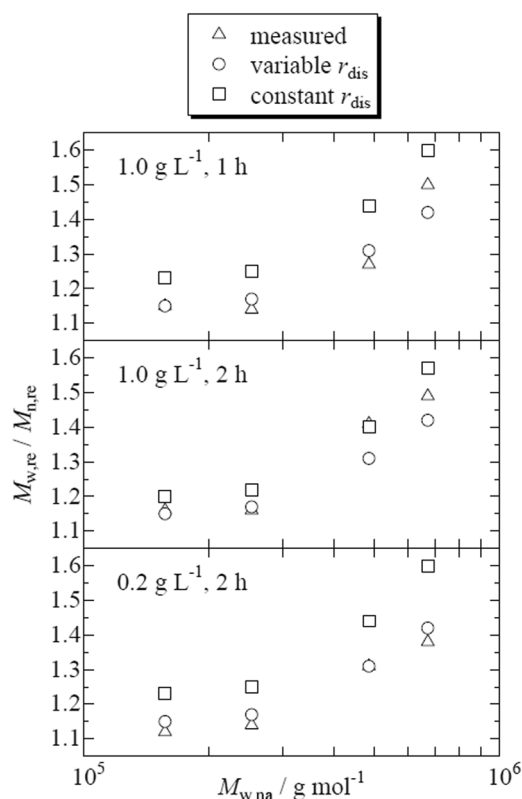


**Fig. 8** Molar mass distribution indices of renatured xanthan determined by a SEC measurement and those calculated by assuming variable  $r_{\text{dis}}$  and constant  $r_{\text{dis}}$ . The concentration of xanthan at the denaturation and renaturation, and the heating times are indicated in the figure

The results in this paper and our previous papers [9, 10, 17] indicates that the denaturation and renaturation behaviors of xanthan are not uniform, but changeable by many factors such as the concentration and molar mass of xanthan. The temperature and pH of solution, which were fixed in this study, can also change the denaturation and renaturation behaviors of xanthan. The denaturation and renaturation behaviors of xanthan should be discussed with respect to the differences in the solution conditions. For the conditions, which we investigated in this paper and our previous paper [17], the change induced by the denaturation and renaturation was not drastic for xanthan used industrially (molar mass of  $\sim 10^7 \text{ g mol}^{-1}$ ). The stability of the dimension and viscosity enhancement to the thermal denaturation and renaturation of xanthan with high molar mass can be an advantage for using xanthan as a viscosity enhancer.

**Acknowledgements** We thank Prof. Takahiro Sato at Department of Macromolecular Science, Osaka University who kindly provided the xanthan samples, allowed us to use the CD instrument, and advised us about the stability of the hairpin structure. This work is partially supported by grants from The Japan Health Foundation and Mishima Kaiun Memorial Foundation.

## Compliance with ethical standards

**Conflict of interest** The authors declare that they have no conflict of interest.

## References

1. Norisuye T, Teramoto A. Polymeric materials encyclopedia. In: Salamone JC, editor. Boca Raton, RC Press; 1996. p. 8801–9.
2. Sato T, Norisuye T, Fujita H. Double-stranded helix of xanthan in dilute solution: evidence from light scattering. *Polym J*. 1984;16:341–50.
3. Sato T, Kojima S, Norisuye T, Fujita H. Double-stranded helix of xanthan in dilute solution: further evidence. *Polym J*. 1984;16:423–9.
4. Sato T, Norisuye T, Fujita H. Double-stranded helix of xanthan in dilute solution: dimensional and hydrodynamic properties in 0.1 M aqueous sodium chloride. *Macromolecules*. 1984;17:2696–700.
5. Liu W, Sato T, Norisuye T, Fujita H. Thermally induced conformational change of xanthan in 0.01 M aqueous sodium chloride. *Carbohyd Res*. 1987;160:267–81.
6. Liu W, Norisuye T. Order-disorder conformation change of xanthan in 0.01 m aqueous sodium chloride: dimensional behavior. *Biopolymers*. 1988;27:1641–54.
7. Capron G, Brigand G, Muller G. About the native and renatured conformation of xanthan exopolysaccharide. *Polymer*. 1997;38:5289–95.
8. Oviatt HW Jr., Brant DA. Viscoelastic behavior of thermally treated aqueous xanthan solutions in the semidilute concentration regime. *Macromolecules*. 1994;27:2402–8.
9. Matsuda Y, Biyajima Y, Sato T. Thermal denaturation, renaturation, and aggregation of a double-helical polysaccharide xanthan in aqueous solutions. *Polym J*. 2009;41:526–32.
10. Matsuda Y, Sugiura F, Mays JW, Tasaka S. Atomic force microscopy of thermally renatured xanthan with low molar mass. *Polym J*. 2015;47:282–5.
11. Mohri K, Nishikawa M, Takahashi N, Shiomi T, Matsuoka N, Ogawa K, Endo M, Hidaka K, Sugiyama H, Takahashi Y, Takakura Y. Design and development of nanosized DNA assemblies in polypod-like structure as efficient vehicles for immunostimulatory CpG motifs to immune cells. *ACS Nano*. 2012;6:5931–40.
12. Osada K, Oshima H, Kobayashi D, Doi M, Enoki M, Yamasaki Y, Kataoka K. Quantized folding of plasmid DNA condensed with block cationomer into characteristic rod structure promoting transgene efficacy. *J Am Chem Soc*. 2010;132:12343–8.
13. Choppe E, Puaud F, Nicolai T, Benyahia L. Rheology of xanthan solutions as a function of temperature, concentration and ionic strength. *Carbohyd Polym*. 2010;82:1228–35.
14. Papagiannopoulos A, Sotiropoulos K, Pispas S. Particle tracking microrheology of the power-law viscoelasticity of xanthan solutions. *Food Hydrocoll*. 2016;61:201–10.
15. Ikeda S, Gohtani S, Nishinari K, Zhong Q. Single molecules and networks of xanthan gum probed by atomic force microscopy. *Food Sci Technol Res*. 2012;18:741–5.
16. Moffat J, Morris VJ, Al-Assaf S, Gunning AP. Visualisation of xanthan conformation by atomic force microscopy. *Carbohyd Polym*. 2016;148:380–9.
17. Matsuda Y, Sugiura F, Okumura K, Tasaka S. Renaturation behavior of xanthan with high molar mass and wide molar mass distribution. *Polym J*. 2016;48:653–8.
18. García-Ochoa F, Santos VE, Casas JA, Gómez E. Xanthan gum: production, recovery, and properties. *Biotechnol Adv*. 2000;18:549–79.